TECHNICAL ARTICLE

In situ high-temperature X-ray diffraction studies of reduction of K_2CrO_4 and the formation of K_xCrO_y compounds

Shu-ting Liang,[a,b] Hong-ling Zhang,[a,b,a)] Min-ting Luo,[a,b] Yu-lan Bai,[c] Hong-bin Xu,[a,b] and Yi Zhang[a,b]
[a]*National Engineering Laboratory for Hydrometallurgical Cleaner Production Technology, Institute of Process Engineering, Chinese Academy of Science, Beijing 100190, China*
[b]*Key Laboratory of Green Process and Engineering, Chinese Academy of Sciences, Beijing 100190, China*
[c]*College of Chemistry and Pharmaceutical Sciences, Qingdao Agricultural University, Qingdao 266109, China*

(Received 25 February 2017; accepted 1 June 2017)

In this work, the reduction mechanism of potassium chromate (K_2CrO_4) was investigated via *in situ* high-temperature X-ray diffraction coupled with Fourier transform infrared spectroscopy. During the hydrogen reduction of K_2CrO_4, the formation of K_3CrO_4, $KCrO_2$, and K_xCrO_2 were detected for the first time. The study discovered that K_2CrO_4 was firstly reduced to K_3CrO_4 and an amorphous Cr(III) intermediate product at low temperature (400–500 °C). Moreover, the K_3CrO_4 was the only crystalline material at this stage. As the temperature increased, a stabilized amorphous CrOOH was formed. At a high temperature (550–700 °C), $KCrO_2$ was generated. Interestingly, a portion of $KCrO_2$ was spontaneously decomposed during the hydrogen reduction, accompanying by the formation of $K_{0.7}CrO_2$. Finally, the results clearly illustrated the reduction mechanism of K_2CrO_4: $K_2CrO_4 \rightarrow K_3CrO_4 \rightarrow$ amorphous intermediate $\rightarrow KCrO_2$. © *2017 International Centre for Diffraction Data.*
[doi:10.1017/S0885715617000690]

Key words: *in situ* XRD, *in situ* FTIR, K_2CrO_4, reduction mechanism, activated K_xCrO_y

I. INTRODUCTION

Potassium chromate (K_2CrO_4) is a product extracted from chromite ore through many hydrometallurgical processes (Zheng *et al.*, 2006). It has been used for producing chrome oxide (Cr_2O_3), which was followed by numerous applications such as green pigments (Liang *et al.*, 2014), nano-composite batteries (Abbas *et al.*, 2016), catalysts (Mahmoud, 2016), gas sensors (Park *et al.*, 2015), magnetic materials (Anandan and Rajendran, 2014), and solar energy materials (Khamlich and Maaza, 2015).

The hydrogen reduction of K_2CrO_4 to form Cr(III) compounds is the chief step during the preparation process of Cr_2O_3. In the past, the valence state changes of chromium (Cr) and the corresponding reduction products during the hydrogen reduction of K_2CrO_4 have not been thoroughly researched.

It is well known that potassium and Cr are known to form a number of crystallographically well-defined K_xCrO_y compounds, such as K_3CrO_4 (Johnson, 1978), K_3CrO_8 (Cage *et al.*, 1999), KCr_3O_8 (Vidya *et al.*, 2006), and $KCrO_2$ (Zafar Ali *et al.*, 2013). The reduction products of K_2CrO_4 may contain many Cr^{5+}, Cr^{4+}, and Cr^{3+} compounds. Among them, Cr^{6+} and Cr^{3+} are the most stable states, with stable electronic configurations of d^3 and d^0, respectively (Weckhuysen *et al.*, 1997). While the Cr^{5+} and Cr^{4+} are less stable, the reaction in air involves the disproportionation reaction of Cr^{5+}, which would produce 1/3 of Cr^{3+} and 2/3 of Cr^{6+}.

Primitive works have indicated that the reduction products contain amorphous CrOOH and $KCrO_2$, while there is not sufficient evidence to support the generation of $KCrO_2$ (Bai *et al.*, 2006; Li *et al.*, 2008). Because the unstable $KCrO_2$, Cr^{5+} and Cr^{4+} compounds are extremely sensitive to the air and humidity, they are immediately oxidized in the atmospheric environment (Delmas *et al.*, 1975). Therefore, the $KCrO_2$ and complicated reduction products could not be identified using conventional methods.

The development of *in situ* high-temperature X-ray diffraction (XRD) and *in situ* Fourier transform infrared spectroscopy (FTIR) technology make the structural analyses in a dry and inert atmosphere possible (Sakaki *et al.*, 2011; Kubis *et al.*, 2014). To elucidate the reduction mechanism of K_2CrO_4 and the existence of various K_xCrO_y compounds, *in situ* high-temperature XRD was employed to detect crystalline phases, and *in situ* FTIR was used to measure the amorphous phase. We sought to elucidate the changes of the crystal structure and the composition of products during the reduction process. In addition, the effects of the reduction rate were also studied, including reduction temperature and time.

II. EXPERIMENTS

A. Materials

The K_2CrO_4 (A.R.) used in this work was manufactured via the KOH hydrometallurgical process (Zheng *et al.*, 2006). The purity of the reduction gas (99.9%, v/v) was composed of 3.55% hydrogen and 96.45% helium.

B. *In situ* XRD

In situ XRD experiments were carried out using a SmartLab X-ray diffractometer equipped with a secondary

[a)]Author to whom correspondence should be addressed. Electronic mail: hlzhang@ipe.ac.cn

monochromator (Cu$K\alpha_1$ radiation). The *in situ* cell consisted of a XRK-900 Anton Paar high-temperature reactor chamber (volume of 400 ml), which was mounted onto a goniometer and connected to a gas-feed system (He and H_2).

The content of hydrogen was limited to 4% to avoid the risk of an explosion. K_2CrO_4 was reduced by a mixture of gas (3.55% hydrogen and 96.45% helium) from 30 to 700 °C. The pressure of the mixture gas was 1 atm, and the flow rate was 300 mL min^{-1}. The temperature was measured using a thermocouple contacting with the sample holder. The ambient temperature was controlled using a TCU 750 temperature controller, allowing the maximum temperature of 750 °C. From 30 to 400 °C, the temperature was increased at a rate of 10 °C min^{-1}, and from 400 to 700 °C, the temperature was increased at a rate of 1 °C min^{-1}. The holding time was 10 min before every test. A machinable "Macor" glass ceramic was used as a sample holder. A very small nickel (Ni) boat was placed on the top of the Macor to preventing the Macor contact with the molten reduction product KOH. The appropriate *z*-alignment of the XRK 900 was ensured after changing each sample. The 2θ range was also tested before every experiment.

General XRD patterns were recorded using a Rigaku diffractometer employing Cu$K\alpha$ radiation (from 5° to 90° 2θ at steps of 0.02° 2θ, and a counting time of 2 s $step^{-1}$).

C. *In situ* FTIR

The *in situ* FTIR experiments were performed using a Nicolet 6700 FTIR spectrometer equipped with a DTGS detector. The pure K_2CrO_4 sample that underwent the infrared (IR) analysis were pressed to a self-supporting wafer (60–100 mg). This wafer was then sealed with stainless steel gaskets. The samples were heated to 600 °C in a flowing stream (30 mL min^{-1}) of 3.55% hydrogen and 96.45% helium. From 30 to 600 °C, the temperature was increased at 10 °C min^{-1}. After the signals were stable at each temperature, the IR spectra were obtained. The IR spectra were recorded at a resolution of 3 cm^{-1} using 250 signal-averaged scans.

III. RESULTS AND DISCUSSION

A. *In situ* XRD

The first *in situ* powder XRD experiment was performed using hydrogen as the reducing agent (3.55 vol.% H_2 blanched with He, 300 mL min^{-1}). The results are presented in Figure 1.

When the temperature was increased, from 30 to 480 °C, the K_2CrO_4 was reduced by hydrogen. The diffraction peaks of K_2CrO_4 gradually decreased, and shifted to lower angles (shown in broken line). This is because with the enhancement of temperatures, the interplanar spacing of K_2CrO_4 becomes larger. At 480 °C, the K_3CrO_4 was observed. When the system was further heated to 500 °C, the diffraction peaks of K_3CrO_4 disappeared, and the amorphous intermediate was observed. Above 560 °C, the formation of $KCrO_2$ was observed. A mixture of $KCrO_2$ and K_xCrO_2 was obtained at temperatures from 600 to 700 °C.

The crystalline phases were identified via the international center for diffraction data files (K_2CrO_4, PDF No. 00-15-0365; K_3CrO_4, PDF No. 00-31-0994; $KCrO_2$, PDF No. 00-46-0262; K_xCrO_2, PDF No. 04-020-6422; Ni, PDF No. 00-04-0850). The corresponding lattice parameters of different reduction products, including K_3CrO_4, $KCrO_2$, and $K_{0.7}CrO_2$ are presented in Table I. The XRD patterns of the reduction products at 480, 520, and 660 °C are also presented in Figure S1 (Supporting Information).

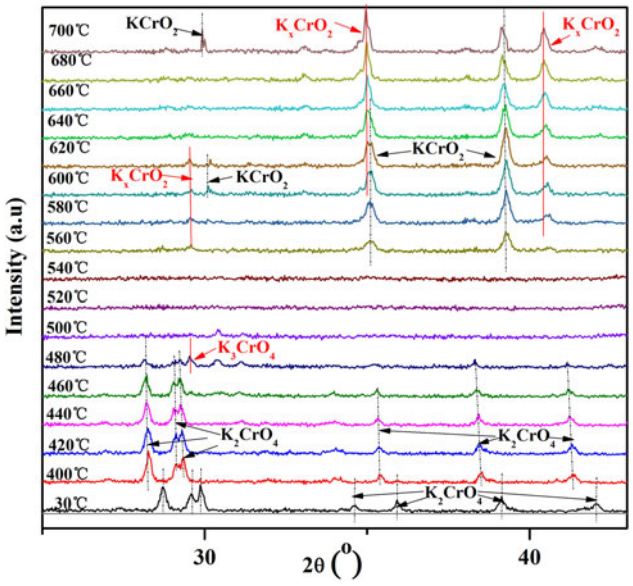

Figure 1. (Color online) Evolution of XRD patterns during the reduction of K_2CrO_4 from 30 to 700 °C. Characteristic diffraction lines of K_2CrO_4, K_3CrO_4, and $KCrO_2$ are indicated.

The lowest formation temperatures of the K_3CrO_4, amorphous intermediate and $KCrO_2 + K_xCrO_2$ were 480, 500, and 600 °C, respectively. Thus, the XRD measurements of the reduction reaction of K_2CrO_4 under isothermal conditions were also performed at different temperatures.

Figure 2 show the time-resolved XRD data for the isothermal reduction of K_2CrO_4 at 500 °C (also seen in Figure S2, Supporting Information). These experimental conditions (gas flow rate, 3.55 vol.% H_2 and 96.5 vol.% He) were similar to the above experiment. In the first 2 min, Cr^{6+} is reduced to Cr^{5+}, and K_2CrO_4 is simultaneously reduced to K_3CrO_4. Next, K_3CrO_4 is reduced to forming an amorphous compound. Moreover, the final reduction product was an amorphous intermediate at a low temperature of 500 °C.

Figure 3 shows the data for the isothermal reduction of the K_2CrO_4 powders at 600 °C. In this experiment, the onset of K_3CrO_4 and the amorphous intermediate phase transition were also observed. After an "amorphous period" of approximately 30 min, the formation of crystalline phases K_xCrO_2 and $KCrO_2$ were observed in this stage. The XRD peaks of K_3CrO_4, $KCrO_2$, and $KCrO_2 + K_xCrO_2$ during reduction at 600 °C for various durations were also show in Figure S3 (Supporting Information).

TABLE I. The corresponding lattice parameters of different reduction products from 30 to 700 °C.

Temperature (°C)	Products	*a* (Å)	*b* (Å)	*c* (Å)
30	K_2CrO_4	7.6897	10.4268	5.9435
400	K_2CrO_4	7.8131	10.5918	6.0424
480	K_3CrO_4	8.3368	8.3368	8.3368
700	$KCrO_2$	3.0562	3.0562	18.0876
700	$K_{0.7}CrO_2$	6.7169	3.0353	5.1613

https://doi.org/10.1017/S0885715617000690 Published online by Cambridge University Press

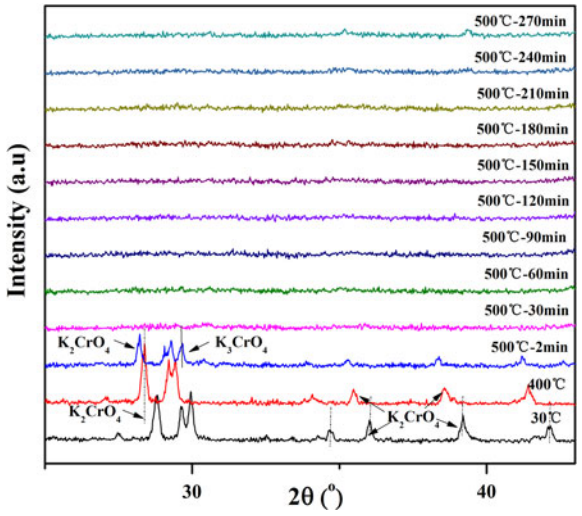

Figure 2. (Color online) Evolution of XRD patterns during the reduction of K_2CrO_4 at 500 °C for 270 min.

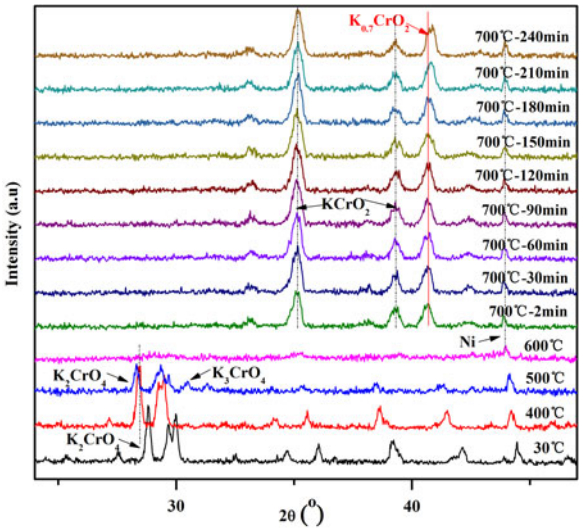

Figure 4. (Color online) Evolution of XRD patterns during the reduction of K_2CrO_4 at 700 °C for 240 min.

According to the XRD analysis shown in Figure 3, the diffraction peaks of K_xCrO_2 were well indexed and in good agreement with the standard PDF No. 04-020-6422, indicating that the resultant material was monoclinic K_xCrO_2 ($0.70 \le x \le 0.77$). In addition, K was also observed during the reduction process. The recorded Ni peak is attributed to the nickel (Ni) boat in the XRD detection.

In situ powder XRD measurements for the isothermal reduction of K_2CrO_4 at 700 °C were also performed, and the results are presented in Figure 4 (also seen in Figure S4, Supporting Information). The reduction of K_2CrO_4 directly resulted in the formation of $KCrO_2$ and K_xCrO_2 ($0.70 \le x \le 0.77$) at 700 °C. No additional crystalline phases were detected in this temperature range. Taking these results into account, $KCrO_2$ and K_xCrO_2 ($0.70 \le x \le 0.77$) were the final products of the reduction of K_2CrO_4 at 700 °C.

The *in situ* XRD experiments under isothermal and temperature-programmed reaction conditions indicated that the entire reduction process consisted of three solid solution regions: K_3CrO_4, an amorphous intermediate, and $KCrO_2 + K_{0.7}CrO_2$. The detail reduction mechanism is discussed; and it was discovered that during the reduction of K_2CrO_4, a three-step process was obvious:

$$K_2CrO_4 \rightarrow K_3CrO_4 \rightarrow \text{amorphous intermediate} \rightarrow KCrO_2 + K_xCrO_2. \quad (1)$$

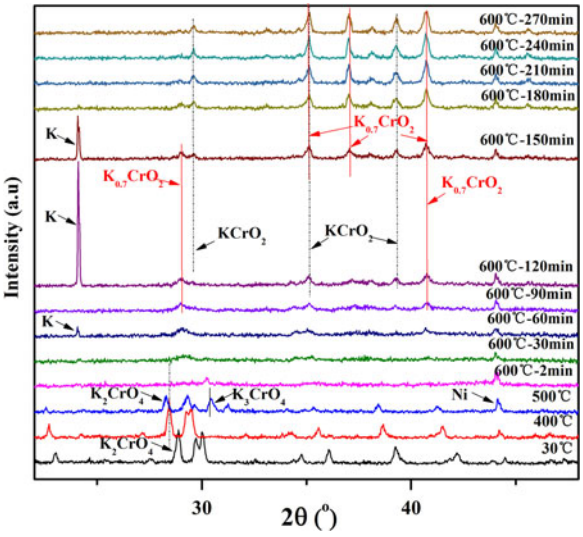

Figure 3. (Color online) Evolution of the XRD patterns during the reduction of K_2CrO_4 at 600 °C for 270 min.

During the hydrogen reduction of K_2CrO_4, diffraction peaks for K_3CrO_4, $KCrO_2$, and K_xCrO_2 were discovered for the first time. The oxidation state of Cr^{5+} was rather unstable. The dark-green K_3CrO_4 is highly hygroscopic and sensitive, and it is spontaneously oxidized when exposed to air at room temperature. For the typical route to synthesizing K_3CrO_4, Cr_2O_3, KOH, and K_2CrO_4 were used as the raw materials, and the reaction was completed at 700 °C in approximately 8 h (Banks and Jaunarajs, 1965; Scholder *et al.*, 1968; Bamberger and Richardson, 1975). However, in this work, K_3CrO_4 was prepared through a simple and low-temperature method.

$KCrO_2$ is a green powder with a magnetic property, and it is extremely sensitive to moisture and oxygen as well (Zafar Ali *et al.*, 2013). In the past, $KCrO_2$ has been synthesized via an azide/nitrate route (Delmas *et al.*, 1975; Scheld and Hoppe, 1989; Delmas *et al.*, 2007). This method must be executed at high-temperature and dangerous pressures. Using the facile and highly reproducible hydrogen reduction method, $KCrO_2$ was first prepared.

The mechanism of the generation of $KCrO_2$ and K_xCrO_2 was discovered as well. It was reported that K_xCrO_2 can be crystallized in two polymorphs, K_xCrO_2 ($0.70 \le x \le 0.77$) and K_xCrO_2 ($0.50 \le x \le 0.60$) (Delmas *et al.*, 1975). $K_{0.7}CrO_2$, PDF No. 04-020-6422, was crystallized in a monoclinic system [$A2/m$; $a = 6.581$ Å, $b = 2.986$ Å, $c = 5.062$ Å]. While $K_{0.5}CrO_2$, PDF No. 00-028-0745, crystallizes in a rhombohedral system [$R3m$; $a = 2.918$ Å, $b = 2.918$ Å, $c = 18.840$ Å]. Delmas has reported that the pure $KCrO_2$ evolves metal potassium in vacuum at high temperatures, and the

https://doi.org/10.1017/S0885715617000690 Published online by Cambridge University Press

reactions can be described by the following equations (Delmas *et al.*, 2007):

$$KCrO_2 = K_xCrO_2 + (1-x)K \uparrow (0.70 \le x \le 0.77) \quad (2)$$

$$KCrO_2 = K_xCrO_2 + (1-x)K \uparrow (0.50 \le x \le 0.60) \quad (3)$$

When the temperature is 700 °C, a potassium-deficient phase with the formula $K_{0.7}CrO_2$ is obtained (Delmas *et al.*, 2007). When the temperature is raised to 900 °C, a phase more deficient in potassium $K_{0.5}CrO_2$ is obtained. $K_{0.7}CrO_2$ and $K_{0.5}CrO_2$ are very sensitive to moisture and oxygen. Zhou *et al*. have also suggested that the electrode of $NaCrO_2$ can be break down into $Na_{0.75}CrO_2$ and $Na_{0.5}CrO_2$ during the battery charging (Zhou *et al.*, 2013), which was in fair agreement with the potassium extraction of $KCrO_2$.

This result demonstrated that the formation of the $K_{0.7}CrO_2$ and metal K was because of the decomposition of the $KCrO_2$ under a dry and helium atmosphere. In addition, some of the reduction products were liable to spontaneously combustible after they were in contact with water, which also proved that the metal K may exist in reduction products.

The onset of the $KCrO_2$ and K_xCrO_2 ($0.70 \le x \le 0.77$) phase transition at 600 °C was also observed, and shown in Figure 5. The peak at $2\theta = 39.290°$ was assigned to d (1 0 4) diffraction of the $KCrO_2$ phase, whereas the peak at $2\theta = 40.808°$ was assigned to d (1 1 1) diffraction of the $K_{0.7}CrO_2$ phase. As shown in Figure 5, both $KCrO_2$ and $K_{0.7}CrO_2$ were present almost simultaneously. The intensity of the two diffraction lines increased with prolonging the times. During the reduction of K_2CrO_4 at a high temperature, $KCrO_2$ was produced and decomposed spontaneously into $K_{0.7}CrO_2$ and metal K.

B. *In situ* FTIR spectroscopy

Some amorphous materials were generated during the reduction reaction. To characterize the amorphous phase, the *in situ* FTIR studies of hydrogen reduction at different temperatures were also performed.

The experiment was performed using hydrogen (3.55 vol. % H_2 in helium) as the reducing agent. The reduction results during 30 to 600 °C are presented in Figure 6(a). The specific changes of the different reduction products at 30–600 °C are presented in Figures 6(b)–(f). The IR spectroscopy of pure K_2CrO_4, KOH, and CrOOH are presented as the reference samples in Figure 6(g).

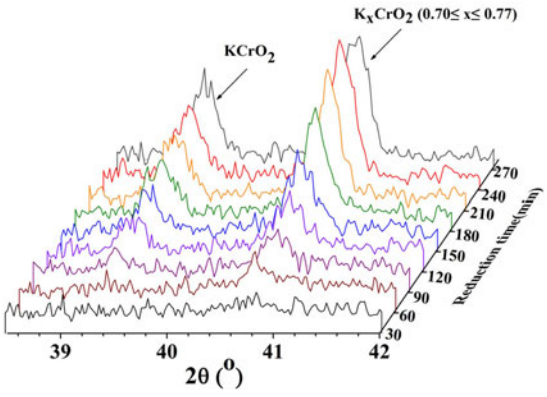

Figure 5. (Color online) The phase of $KCrO_2$ and K_xCrO_2 ($0.70 \le x \le 0.77$) increased with prolonging reduction time at 600 °C.

The three upward bands at 883, 1228, and 1759 cm^{-1} are assigned to K_2CrO_4 (Miller and Wilkins, 1952; Campbell, 1965). When the reduction temperature was increased from 400 to 560 °C, two downward bands were observed at 505 and 1384 cm^{-1}, which were attributed to the Cr^{III}–O stretching modes (Marshall *et al.*, 1965; Yang *et al.*, 2011) and KOH (Russell, 1979), respectively. The experimental phenomena indicate that K_2CrO_4 (Cr^{6+}) is preferentially reduced to a high activity Cr^{3+} compound and KOH.

After the reduction temperature is increased to 570 °C, two downward bands were observed at 505 and 1384 cm^{-1}, which attributed to Cr^{III}–O stretching modes and KOH, respectively. A downward band was found at 638–630 cm^{-1}, which is assigned to groups of the CrO_4^{x-} type, where $x = 3$ (Bailey and Symons, 1957; Ratnasamy and Leonard, 1972). This band was detected as crystalline K_3CrO_4 in the *in situ* XRD. However, the band at approximately 850 cm^{-1} was also assigned to the linearly bonder of $\upsilon(Cr^{VI}–O)$ (Muller *et al.*, 1969), which indicates that Cr^{6+} also existed in the reduction product at 570 °C. Therefore, Cr^{3+}, Cr^{5+}, and Cr^{6+} coexist in the reduction product at this stage.

When the reduction temperature is increased to 580–600 °C, the reduction products clearly show four bands: 536, 1105, 1390, and 1720 cm^{-1}. The strong sharp peak at 539 cm^{-1} corresponds to the Cr^{III}–O anti-symmetric stretching vibration (Yang *et al.*, 2010; Yang *et al.*, 2011). The band at approximately 1105 cm^{-1} corresponds to the linearly bonder of $\delta(Cr^{III}–O–H)$ (Russell, 1979). These bands are characteristic of CrOOH (Snyder and Ibers, 1962; Ratnasamy and Leonard, 1972; Bai *et al.*, 2006). In addition, the low-intensity band observed at 1720 cm^{-1} is assigned to the bending modes of non-dissociated water molecules (Pei *et al.*, 2009), and the downward band at 1390 cm^{-1} is assigned to KOH ($\upsilon_{O–H}$). The FTIR studies discussed above demonstrate that amorphous CrOOH and KOH are the main phase products in the amorphous intermediate solid solution region. Furthermore, the band at approximately 850 cm^{-1}, which would be assigned to the linearly bonder of $\upsilon(Cr^{VI}–O)$, was not found, indicating that Cr^{6+} is completely reduced at 580 °C.

Table II shows different dominant peaks of the reduction products. According to the related peak intensities changes, the high-activity Cr^{3+} compound and KOH are the main phase products of the primary stage of reduction. With increasing reduction times, crystalline K_3CrO_4 was generated. At a higher temperature of 600 °C, the K_2CrO_4 and K_3CrO_4 were completely reduced to Cr^{3+} compound, and amorphous CrOOH and KOH are the main phase products in the amorphous intermediate region.

C. Reduction mechanism

To summarize the above-discussed *in situ* XRD and FTIR results, we propose that the hydrogen reduction of K_2CrO_4 is a very complex process. Increasing the reaction temperatures and times were beneficial for the reduction.

From 30 to 500 °C, according to the experimental results of FTIR, the K_2CrO_4 was preferentially but incompletely reduced to Cr^{3+} and KOH. As the reduction proceeded, amorphous Cr^{3+} compound chemically reacted with KOH and K_2CrO_4 to form higher oxidation states of Cr. The XRD

https://doi.org/10.1017/S0885715617000690 Published online by Cambridge University Press

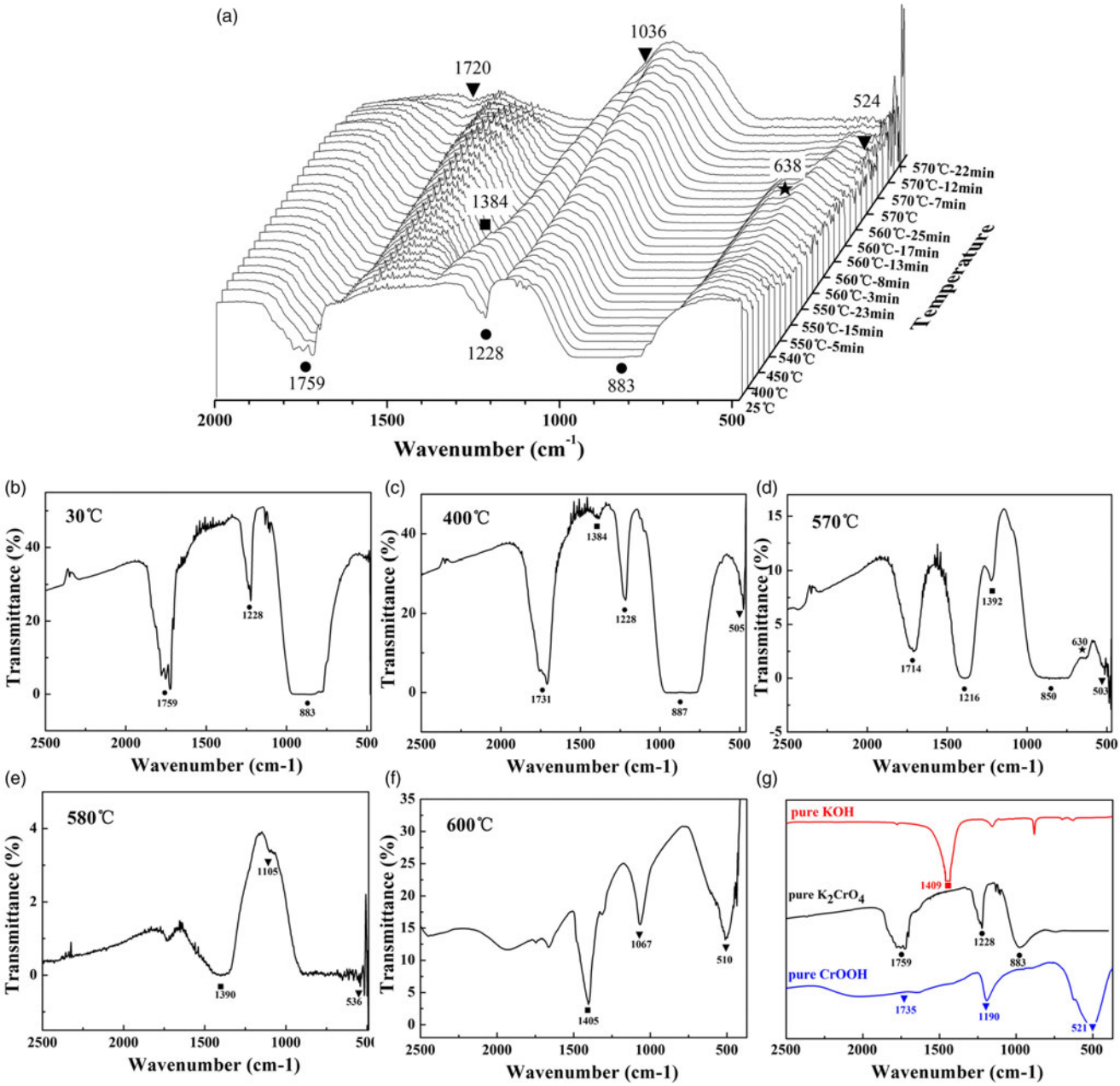

Figure 6. (Color online) (a) Evolution of IR spectroscopy during the reduction of K_2CrO_4 in hydrogen from 30 to 570 °C; (b) The IR spectroscopy of the reduction product at 30 °C; (c) The IR spectroscopy of the reduction product at 400 °C; (d) The IR spectroscopy of the reduction product at 570 °C; (e) The IR spectroscopy of the reduction product at 580 °C; (f) The IR spectroscopy of the reduction product at 600 °C; (g) IR spectroscopy of pure K_2CrO_4, KOH, and CrOOH; ●$\upsilon(K_2CrO_4)$ = 883, 1228, 1759 cm^{-1}; ■υ(KOH) = 1409 cm^{-1}; ★$\upsilon(K_3CrO_4)$ = 630–638 cm^{-1}; ▼υ(CrOOH) = 521, 1190, 1735 cm^{-1}.

experimental results showed that the Cr^{5+} compound was K_3CrO_4 without the formation of other crystalline phases. Cr^{3+}, Cr^{5+}, and Cr^{6+} coexisted at this stage.

From 500 to 600 °C, as the reduction proceeded, Cr^{6+} was completely reduced. XRD results indicated that amorphous intermediate was the final product of the reduction of K_2CrO_4. Considering the IR spectrum, the main phase products in the amorphous intermediate region were amorphous CrOOH and KOH. The KOH became amorphous molten substances above 406 °C.

Above 600 °C, the formation of $KCrO_2$ was observed. In addition, $KCrO_2$ was the only product formed during the reduction of K_2CrO_4. None of the other crystallographically compounds were detected. According to previous experimental results, $KCrO_2$ may be formed by the reaction of the newly produced amorphous CrOOH and KOH (Bai *et al.*, 2006). In addition, if the reaction time was extended, $KCrO_2$ may be partial decomposed into the K_xCrO_2 ($0.70 \le x \le 0.77$) and K metal phases. At a higher reaction temperature of 700 °C, the formation of $KCrO_2$ and $K_{0.7}CrO_2$ were immediately observed. Therefore, it was concluded that the reduction proceeds following a consecutive mechanism: CrOOH and KOH first react to form $KCrO_2$, and then $KCrO_2$ is decomposed partially but immediately into the $K_{0.7}CrO_2$ and K metal phases. The two reaction fronts coexist simultaneously.

https://doi.org/10.1017/S0885715617000690 Published online by Cambridge University Press

TABLE II. The IR spectrum of different reduction products during reduction of K_2CrO_4 from 30 to 600 °C.

	IR spectrum (cm^{-1})						
Temperature (°C)	$\upsilon(Cr^{III}–O)$	$\upsilon(Cr^{V}–O)$	$\upsilon(Cr^{VI}–O)$	$\delta(Cr^{III}–O–H)$	$\upsilon(CrO_4^{2-})$	υ(HKO)	δ(H–O)
30	–	–	883	–	1228	–	1759
400	505	–	887	–	1228	1384	1731
450	493	–	871	–	1226	1378	1732
500	492	–	860	–	1222	1378	1726
550	498	–	860	–	1224	1377	1730
560	514	638	852	–	1216	1390	1714
570	503	630	850	–	1216	1392	1714
580	536	–	–	1105	–	1390	1720
600	524	–	–	1036	–	1457	–
K_2CrO_4	–	–	883	–	1228	–	1759
KOH	–	–	–	–	–	1409	–
CrOOH	521	–	–	1190	–	–	1735

Hence, the reaction can be described by the following processes:

$$K_2CrO_4 \rightarrow \text{amorphous } Cr^{3+} + K_3CrO_4 \rightarrow \text{amorphous CrOOH} \rightarrow KCrO_2 \quad (4)$$

In the final heating stage, $KCrO_2$ spontaneous decomposed. The different stages of the reaction are:

$$7K_2CrO_4 + 5H_2 \rightarrow 4 \text{ amorphous } Cr^{3+} \text{ compound} + 3K_3CrO_4 + 5/2H_2O \quad (30 \text{ to } 500\ ^{\circ}C) \quad (5)$$

$$2K_2CrO_4 + 3H_2 \rightarrow 2 \text{ amorphous CrOOH} + 4KOH \quad (500 \text{ to } 600\ ^{\circ}C) \quad (6)$$

$$CrOOH + KOH \rightarrow KCrO_2 + H_2O \quad (> 600\ ^{\circ}C) \quad (7)$$

$$KCrO_2 \rightarrow K_xCrO_2 + (1-x)K \uparrow \ (0.70 \le x \le 0.77) \quad (> 600\ ^{\circ}C \text{ parallel reaction}) \quad (8)$$

IV. CONCLUSIONS

Here, we report that the hydrogen reduction of K_2CrO_4 using *in situ* high-temperature XRD and *in situ* FTIR in the protection of the inert atmosphere. The mechanisms involved were interpreted that the hydrogen reduction of K_2CrO_4 was a consecutive reaction ($K_2CrO_4 \rightarrow$ amorphous $Cr^{3+} + K_3CrO_4 \rightarrow$ amorphous CrOOH $\rightarrow KCrO_2$) with many intermediate products, including K_3CrO_4, amorphous CrOOH, $KCrO_2$, and $K_{0.7}CrO_2$. The effects of the reduction temperature and time on the control of the reduction products were clarified. Such mechanisms are hard to achieve on the conventional reduction methods. The present finding has both fundamental and practical significance. For example, they suggest a generalized way of simultaneous making very rare K_3CrO_4, $KCrO_2$, and $K_{0.7}CrO_2$ materials, which have been found to possess unique high-activity and antiferromagnetic virtues in a wide variety of important areas. Besides, this reduction mechanism is also a good reference to the other reduction process of chromate, such as X_2CrO_4 phases (X = Na and K).

SUPPLEMENTARY MATERIAL

The supplementary material for this article can be found at https://doi.org/10.1017/S0885715617000690

ACKNOWLEDGMENTS

The authors gratefully acknowledge financial support from the National Natural Science Foundation of China (Grant No. 11204304), the National Basic Research Program (973 Program) of China (Grant No. 2013CB632600), and the National High-tech Research and Development Program of China (Grant No. 2011AA060702).

Abbas, S. M., Ahmad, N., Rehman, A. U., Rana, U. A., Khan, S. U., Hussain, S., and Nam, K. W. (**2016**). "High rate capability and long cycle stability of Cr_2O_3 anode with CNTs for lithium ion batteries," Electrochim. Acta **212**, 260–269.

Anandan, K. and Rajendran, V. (**2014**). "Studies on structural, morphological, magnetic and optical properties of chromium sesquioxide (Cr_2O_3) nanoparticles: synthesized via facile solvothermal process by different solvents," Mater. Sci. Semicond. Proc. **19**, 136–144.

Bai, Y. L., Xu, H. B., Zhang, Y., and Li, Z. H. (**2006**). "Reductive conversion of hexavalent chromium in the preparation of ultra-fine chromia powder," J. Phys. Chem. Solids **67**, 2589–2595.

Bailey, N. and Symons, M. C. R. (**1957**). "Structure and reactivity of the oxyanions of transition metals. Part III. The hypochromate ion," J. Chem. Soc. **1**, 203–207.

Bamberger, C. E. and Richardson, D. M. (**1975**). "Chemical cycle for thermochemical production of hydrogen from water," US 3927192.

Banks, E. and Jaunarajs, K. L. (**1965**). "Chromium analogs of apatite and spodiosite," Inorg. Chem. **4**, 78–83.

Cage, B., Weekley, A., Brunel, L. C., and Dalal, N. S. (**1999**). "K_3CrO_8 in K_3NbO_8 as a proposed standard for g-factor, spin concentration, and field calibration in high-field EPR spectroscopy," Anal. Chem. **71**, 1951–1957.

Campbell, J. A. (**1965**). "Spectral evidence for interionic forces in crystal – chromates and dichromates," Spectrochim. Acta **21**, 1333–1343.

Delmas, C., Devalette, M., Fouassier, C., and Hagenmuller, P. (**1975**). "Les phases $KXCrO_2$ ($X < 1$)," Mater. Res. Bull. **10**, 393–398.

Delmas, C., Fouassier, C., Hagenmuller, P., and Ackerman, J. F. (**2007**). "The alkali ternary oxides $AxCoO_2$ and $AxCrO_2$ (A = Na, K)," Inorg. Synth. **22**, 56–61.

Johnson, L. H., Hepler, L. G., Bamberger, C. E., and Richardson, D. M. (**1978**). "The enthalpy of formation of potassium chromate (V), K_3CrO_4 (C)," Can. J. Chem. **56**, 446–449.

Khamlich, S. and Maaza, M. (**2015**). "Cr/α-Cr_2O_3 monodispersed mesospherical particles for mid-temperature solar absorber application," Energy Proc. **68**, 31–36.

Kubis, C., Baumann, W., Barsch, E., Selent, D., Sawall, M., Ludwig, R., Neymeyr, K., Hess, D., Franke, R., and Börner, A. (**2014**). "Investigation into the equilibrium of iridium catalysts for the hydroformylation of olefins by combining *in situ* high-pressure FTIR and NMR spectroscopy," ACS Catal. **4**, 2097–2108.

Li, P., Xu, H. B., Zheng, S. L., Zhang, Y., Li, Z. H., and Bai, Y. L. (**2008**). "A green process to prepare chromic oxide green pigment," Environ. Sci. Technol. **42**, 7231–7235.

Liang, S. T., Zhang, H. L., Luo, M. T., Luo, K. J., Li, P., Xu, H. B., and Zhang, Y. (**2014**). "Colour performance investigation of a Cr_2O_3 green pigment prepared via the thermal decomposition of CrOOH," Ceram. Int. **40**, 4367–4373.

Mahmoud, H. R. (**2016**). "Novel mesoporous Gd^{3+} doped Cr_2O_3 nanomaterials: synthesis, characterization, catalytic and antitumor applications," Adv. Powder. Technol. **27**, 1446–1452.

Marshall, R., Mitra, S. S., Gielisse, P. J., Plendl, J. N., and Mansur, L. C. (**1965**). "Infrared lattice spectra of α-Al_2O_3 and Cr_2O_3," J. Chem. Phys. **43**, 2893–2894.

Miller, F. A. and Wilkins, C. H. (**1952**). "Infrared spectra and characteristic frequencies of inorganic ions," Anal. Chem. **24**, 1253–1294.

Muller, O., White, W. B., and Roy, R. (**1969**). "Infrared spectra of the chromates of magnesium, nickel and cadmium," Spectrochim. Acta A **25**, 1491–1499.

Park, S., Kim, S., Sun, G. J., Choi, S., Lee, S., and Lee, C. (**2015**). "Ethanol sensing properties of networked In_2O_3 nanorods decorated with Cr_2O_3-nanoparticles," Ceram. Int. **41**, 9823–9827.

Pei, Z., Xu, H., and Zhang, Y. (**2009**). "Preparation of Cr_2O_3 nanoparticles via C_2H_5OH hydrothermal reduction," J. Alloy. Compd. **468**, L5–L8.

Ratnasamy, P. and Leonard, A. J. (**1972**). "Structural evolution of chromia," J. Phys. Chem. **76**, 1838–1843.

Russell, J. D. (**1979**). "An infrared spectroscopic study of the interaction of nontronite and ferruginous montmorillonites with alkali metal hydroxides," Clay Miner. **14**, 127–138.

Sakaki, K., Terashita, N., Tsunokake, S., Nakamura, Y., and Akiba, E. (**2011**). "*In situ* X-ray diffraction study of phase transformation of $Mg_{2-x}Pr_xNi_4$ during hydrogenation and dehydrogenation ($x = 0.6$ and 1.0)," J. Phys. Chem. **116**, 1401–1407.

Scheld, W. and Hoppe, R. (**1989**). "Über den α-$NaFeO_2$-Typ: zur Kenntnis von $NaCrO_2$ und $KCrO_2$," Z. Anorg. Allg. Chem. **568**, 151–156.

Scholder, R., Schwochow, F., and Schwarz, H. (**1968**). "Über alkalichromate (V)," Z. Anorg. Allg. Chem. **363**, 10–23.

Snyder, R. G. and Ibers, J. A. (**1962**). "O–H–O and O–D–O potential energy curves for chromous acid," J. Phys. Chem. **36**, 1356–1360.

Vidya, R., Ravindran, P., Kjekshus, A., and Fjellvåg, H. (**2006**). "First-principles density-functional calculations on HCr_3O_8: an exercise to better understand the ACr_3O_8 (A = alkali metal) family," J Electroceram. **17**, 15–20.

Weckhuysen, B. M., Wachs, I. E., and Schoonheydt, R. A. (**1997**). "ChemInform abstract: surface chemistry and spectroscopy of chromium in inorganic oxides," J. Cheminform. **28**, 1.

Yang, J., Martens, W. N., and Frost, R. L. (**2010**). "Transition of chromium oxyhydroxide nanomaterials to chromium oxide: a hot-stage Raman spectroscopic study," J. Raman Spectrosc. **42**, 1142–1146.

Yang, J., Cheng, H., Martens, W. N., and Frost, R. L. (**2011**). "Transition of synthetic chromium oxide gel to crystalline chromium oxide: a hot-stage Raman spectroscopic study," J. Raman Spectrosc. **42**, 1069–1074.

Zafar Ali, N., Nuss, J., and Jansen, M. (**2013**). "A new polymorph of potassium chromate(III), β-$KCrO_2$, and reinvestigation of α-$KCrO_2$," Z. Anorg. Allg. Chem. **639**, 241–245.

Zheng, S., Zhang, Y., Li, Z., Qi, T., Li, H., and Xu, H. (**2006**). "Green metallurgical processing of chromite," Hydrometallurgy **82**, 157–163.

Zhou, Y. N., Ding, J. J., Nam, K. W., Yu, X., Bak, S. M., Hu, E., Liu, J., Bai, J., Li, H., Fu, Z. W., and Yang, X. Q. (**2013**). "Phase transition behavior of $NaCrO_2$ during sodium extraction studied by synchrotron-based X-ray diffraction and absorption spectroscopy," J. Mater. Chem. **1**, 11130–11134.

https://doi.org/10.1017/S0885715617000690 Published online by Cambridge University Press